SEBHA UNIVERSITY JOURNAL OF PURE & APPLIED SCIENCES VOL.23 NO. 1 2024
DOI: 10.51984/JOPAS.V23I1.2910

مجلة جامعة سبها للعلوم البحتة والتطبيقية
Sebha University Journal of Pure & Applied Sciences
Journal homepage: www.sebhau.edu.ly/journal/jopas

Study on Natural Diatomite as an Adsorbent for Uranyl (VI) ions, Using Spectrophotometric Method

*Ragiab A. M. Issa[1], Hana B. AlHanash[2], Mona M. Abdulsalam[3], Amar A. Tekalli[3], Laila K. Ben Hamed[1], and Suha A. Ben Omran[1].

[1] Chemistry Department, Faculty of Education, University of Tripoli
[2] Libyan Advanced Centre for Chemical Analysis
[3] Industrial Research Centre, Tripoli Libya

Keywords:
8-hydroxyquinoline
Diatomite
Spectrophotometric
Uranyl ion
Uptake

ABSTRACT

This work is based on the investigation of uranyl (VI) ion adsorption onto natural diatomite using batch sorption method under different parameters such as pH, initial ion concentration, adsorbent amount and effect of sulfate ion as a foreign ion. 8-hydroxyquinoline is used as a chromogen forming a pale-yellow complex with UO_2^{2+} ions in chloroform, the absorbance was measured spectrophotometrically at λ_{max} 460 nm, obtaining a linear calibration curve with R^2=0.998, LOD=3.03 mg/L and LOQ=9.21 mg/L. Prior to the implementation of the batch experiment, the morphology and composition of diatomite was confirmed using XRF (Bruker S8 Tiger), XRD (Bruker D5005), FTIR (Bruker Vector 22), and SEM (JEOL JSM-5610 LV) techniques. From spectrophotometric analysis, the results showed that the maximum uranyl ion adsorption distribution coefficient reached at the initial concentration of 50ppm, pH 4.5, contact time 5hrs and adsorption dosage of 2 g/L. There was no significant effect of sulfate ion on the adsorption affinity. Adsorption isotherm was studied by Langmuir which was favourable model fitting with R^2=0.996 and maximum adsorption capacity of 16mg/g, and separation factor R_L = 0.0122. Freundlich isotherm model also applied for the same data and give a very straight line with R^2= 1.00 and maximum adsorption capacity of 200 mg/g. Temkin model was less fit and gave a negative isotherm curve with R^2= 0.78, K_T= 0.9405 L/g, b_T= 24.724 J/mol. Langmuir and Freundlich isotherms gave exothermic adsorption while Temkin gave an endothermic one.

دراسة استخدام الدياتوميت الطبيعي كمادة ممتزة لأيونات اليورانيل (VI) باستخدام الطريقة الطيفية

*رجب ع. م. عيسى[1]، هناء ب. ع. الحنش[2]، منى م. عبد السلام[3]، عمار ع. تكالي[3]، ليلى خ. بن حامد[1]، سهى ع. بن عمران[1].

[1] قسم الكيمياء كلية التربية طرابلس جامعة طرابلس.
[2] المركز الليبي المتقدم للتحاليل الكيميائية طرابلس ليبيا.
[3] مركز البحوث الصناعية طرابلس ليبيا.

الكلمات المفتاحية:
أيون اليورانيل
ادمصاص
دياتوميت
8-هيدروكسي كوينولين
قياس الطيف الضوئي

الملخص

يعتمد هذا العمل على دراسة امتزاز أيون اليورانيل (VI) على الدياتوميت الطبيعي باستخدام طريقة إدمصاص بالدفعات باستخدام متغيرات مختلفة مثل الأس الهيدروجيني وتركيز الأيونات الإبتدائي وكمية الممتزات وتأثير أيون الكبريتات كأيون غريب. يستخدم 8-هيدروكسي كوينولين كمادة ملونة تكون معقدا أصفر باهتا مع أيونات UO_2^{2+} في الكلوروفورم، وتم قياس الامتصاص طيفيا عند طول موجي 460 نانومترا، والحصول على منحنى معايرة خطي مع R^2 = 0.998 ، LOD = 3.03 mg/L و LOQ = 9.21 mg/L . تم تشخيص خام الدياتوميت من ناحية التركيب الكيميائي والمرفولوجي قبل اجراء تجارب الامتزاز. باستخدام تقنية الاشعة السينية الوميضية والحيودية، تقنية الاشهة تحت الحمراء، وتقنية المجهر الالكتروني الماسح. من خلال النتائج أتضح أن الحد الأقصى لمعامل توزيع امتزاز أيون اليورانيل وصل عند التركيز الأولي 50 جزء في المليون، ودرجة الحموضة 4.5،

*Corresponding author:
E-mail addresses: ra.issa@uot.edu.ly, (H. B. AlHanash) hanahansh@aal.ly, (M. M. Abdulsalam) mna60061@gmail.com ,(A. A. Tekalli) amar2kalli@yahoo.com, (L. K. Ben Hamed) lailakhlfabenhamed7686758@gmail.com, (S. A. Ben Omran) sohaa4543@gmail.com
Article History : Received 24 December 2023 - Received in revised form 15 March 2024 - Accepted 27 March 2024

وزمن التلامس 5 ساعات وجرعة الامتزاز 2 g/L. لم يكن هناك تأثير معنوي لأيون الكبريتات على كفاءة الامتزاز. تمت دراسة متساوي الحرارة للامتزاز بواسطة Langmuir الذي كان نموذجا مناسبا مع $R^2 = 0.996$ وقدرة امتصاص قصوى تبلغ 16 mg/g، وعامل الفصل $RL = 0.0122$ تم تطبيق نموذج Freundlich isotherm أيضا على نفس البيانات وأعطى خطا مستقيما مع $R^2 = 1.00$ وقدرة امتصاص قصوى تبلغ 200 mg/g. كان نموذج Temkin أقل ملاءمة وأعطى منحنى ماصا للحرارة مع $R^2 = 0.78$ ، $K_T = 0.9405\ L/g$ ، $bT = 24.724 J/mol$. بينما أعطى لنجومر وفرندلش منحنى طاردا للحرار بينما أعطى Temkin امتزازا ماصا للحرارة.

1. Introduction

The rapid growth of contemporary corporations is creating major threats to environmental ecosystems and human health through the creation of contaminants such as: organic pollutants, heavy metals, and radionuclides [1]. Radioactive nuclides enclosed in nuclear waste, such as ^{60}Co, ^{154}Eu, ^{232}Th, ^{235}U, ^{239}Pu, and ^{241}Am, directly contaminate surface water and groundwater sources [2]. Due to their persistent radioactivity, these radionuclides accumulate in food chains and harm human organs via radiation and metabolic reactions [3]. Consequently, public anxiety over the safe disposal of nuclear waste exists [4]. Many methods, such as chemical precipitation [5], ion exchange [6], membrane separation [7], extraction [8] and adsorption [9, 10], have been investigated for extracting and preconcentrating radionuclides from contaminated wastewater [4]. Compared to other methods, adsorption technology is repeatedly used to remove radionuclides from aqueous solutions because of its high efficacy, low cost and ease of use.

Diatoms, which are extremely tiny opaline skeletons of diatomic algae, or their fragments, make up the majority of the light, fine-porous rocks known as diatomites. Diatomites come in a variety of colours, including white, brownish grey, light grey, and yellowish grey. Diatomites sometimes have a dark and brown appearance because they include organic contaminants such as plant remnants. It is appropriate to describe diatoms as nanomaterials because their pores and pore walls frequently have nanoscale dimensions. Each diatomite skeleton has a distinctly organized micro- and nanoporous structure, as shown in photomicrographs [11]. Diatomite has a structure that results in a low density and a strong heat-insulating capacity when compared to other materials with comparable compositions [12]. In this study, natural white diatomite, as received without pretreatment and characterized using XRF (Bruker S8 Tiger), XRD (Bruker D5005), FTIR (Bruker Vector 22), and SEM (JEOL JSM-5610 LV) techniques to assure its composition and morphology. The material was used to study the removal of uranyl ions from aqueous solution following batch experiment techniques. The study was conducted at different pH values, initial ion concentrations and adsorbent amounts. Diatomite was chosen for this work due to its porosity, availability, and density.

2. Experimental work

2.1 Materials

To prepare a stock solution of 1000 ppm UO_2^{2+}, an accurate amount (2.2092 g) of uranyl nitrate hexahydrate, $UO_2(NO_3)_2.6H_2O$ was dissolved in sufficient amount of deionized water and the volume was completed to 1000mL in volumetric flask. A 2.5% solution of 8-hydroxyqunoline (8-HQ) was prepared in chloroform. 0.001, 0.01 and 0.1 N solutions of NaOH and HCl were prepared and used for pH adjustment. Sulphate ion solutions, at concentrations of 2000, 3000 and 4000 ppm of sulfate ion solutions were prepared using potassium sulfate.

2.2 Procedures

A raw diatomite sample was obtained from the Industrial Research Centre, (Tripoli Libya) was manually ground using a porcelain mortar and pestle. The material was passed through a 75-micron sieve and then used without any further treatment. Using a batch experiment method, the adsorption of uranyl ions was studied condsidering the effects of several parameters such as: contact time, pH, initial ion concentration, adsorbate amount and the presence of sulfate ions. Unless stated a 100ppm solution was used for the experiments. The pH was fixed at 4.5 ± 0.05 for all the experiments except for when the effect of pH was studied. The experiments were conducted in 50 mL plastic tubes. Exact amounts of uranyl ions from the 1000ppm solution were transferred to the tubes. Deionized water was added to a final volume 30 mL. The pH was adjusted as required using diluted solutions of HCl and NaOH. After the pH was adjusted, the mixture was adjusted to 40 mL, well shaken after which 0.08±0.0005 g amount of diatomite was added to a final dose of 2g/L for every experiment except where the adsorbent amount was investigated. The tubes were shaken at 80 strokes/minute for 3 hours (with a Memmert water bath), centrifuged for 20 minutes at 4000 rpm (OHAUS) and finally filtered through Whatman filter paper number 41. In a suitable separating flask the remaining uranyl ions were then extracted using four aliquots of a solution of 8-HQ-chloroform (10, 5, 5, 5mL), which were collected together in a 50 mL volumetric flask and completed to the mark with chloroform. Finally, the absorbance was measured at a wavelength of 460nm using a DR 3900 spectrophotometer (HACH). A calibration curve was established by preparing a series of uranyl ion solutions (1.0 – 50.0 mg/L) were prepared by taking exact amounts of uranyl stock solution (1000mg/L) to appropriate separatory funnels (150mL), deionized water was added to make the aqueous phase 50mL. 10mL of 2.5% 8-HQ in chloroform were then added to each funnel. After vigorously shaking, the lower organic layer was carefully separated into 50mL volumetric flask. The aqueous layer remaining in the separatory flask was then treated by three 5mL portions of 8-HQ solution, and the extracts were collected together in the volumetric flask. Finally, the volume was diluted to the mark with chloroform, well shaken and measured spectrophotometrically at λ 460 nm.

3. Results and Discussion

3.1 Mineral characterizations

The diatomite material was characterized by XRF, XRD, IR, and SEM. Table 1 shows that the main components of the diatomite mineral is SiO_2 (87.5%), Al_2O_3 (5.3%), Fe_2O_3 and MgO which account for 1.9% and 1.6% respectively. The Al_2O_3:SiO_2 ratio is 1:16, which verifies that the Al:Si is 1:14. In other words, there is 14.5 moles of Si for each mole of Al. This analysis is compatible with the XRD analysis (Figure. 1)

Table 1 Main chemical composition of the diatomite minerals (XRF analysis).

Content	SiO_2	Al_2O_3	Fe_2O_3	MgO	K_2O
wt %	87.5	5.3	1.9	1.6	0.62
Content	Na_2O	CaO	Ti_2O_3	Cl	
wt %	1.1	0.15	0.24	1.5	

Figure 1 shows a diffractogram of pure diatomite. The main component is SiO_2 which has clear peaks at 19º (4.67 Å), 21º (4.23 Å), 26º (3.42 Å) and 35º (2.56 Å) these are the main diatomite characteristics consistent with previous reports[13]. Figure also shows traces of halite, montmorillonite, and chlorite.

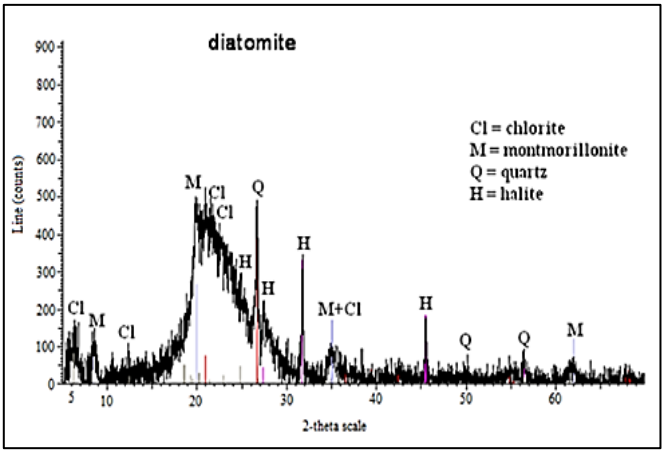

Fig. : XRD diffractogram of pure diatomite.

Figure 2 shows the FTIR spectrum of natural diatomite which highlights a broad peak at 3377 cm^{-1} related to the expansion vibration of hydroxyl groups or water molecules adsorbed on the surface [13]. The spectral bands at wavenumbers 448 cm^{-1} and 1043 cm^{-1} represent the intangible stretch of the Si-O-Si group association, while the peak represents wavenumber of 796 cm^{-1} extensions in the group [14].

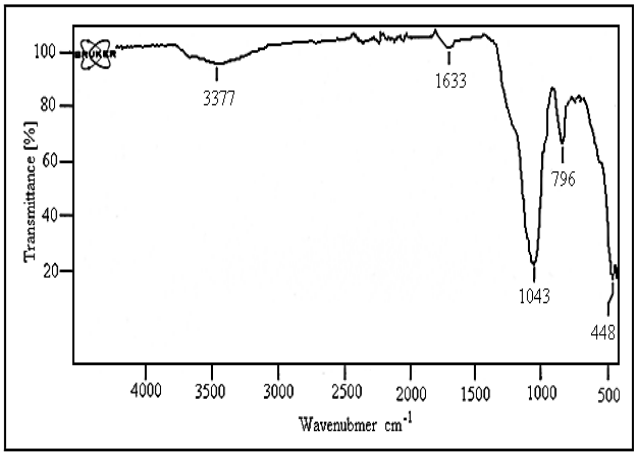

Fig. 2: FTIR spectra for the natural diatomite mineral

Figure 3 shows a SEM image of natural diatomite that was measured using a JEOL JSM.5610LV electron scanning microscope. Diatomite frustules were studied and found to have two types of bumps: centric discoid and pinnate elongated bumps which can clearly appear in the figure [15], [16].

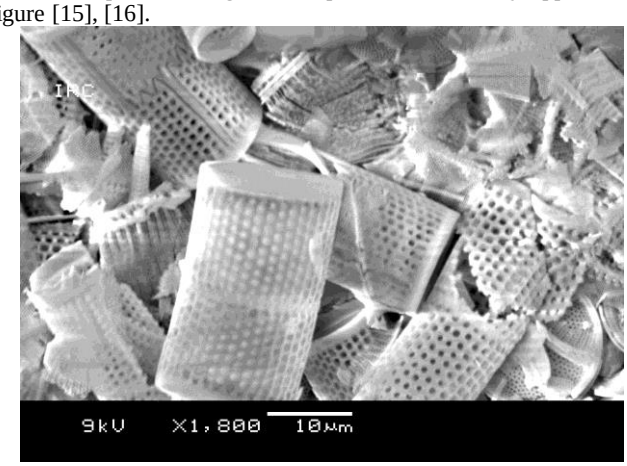

Fig. 3: Scanning electronic microscopy image of natural diatomite

3.2 Calibration curve

As shown in Figure 4, the calibration curve was linear with correlation coefficient R^2 =0.9978.

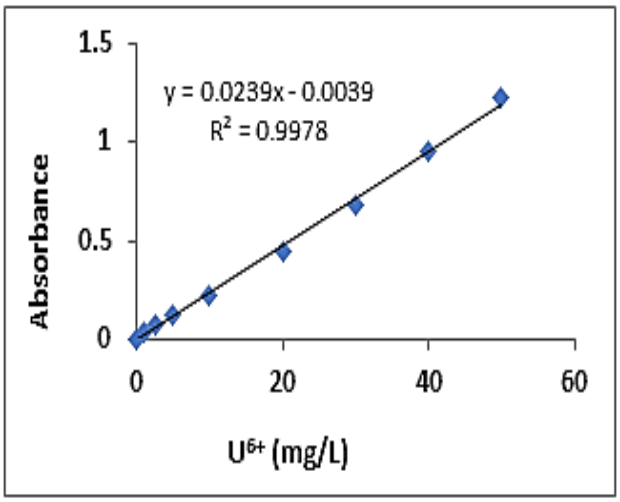

Fig. 4: Calibration curve for standard U^{6+} solution at 1-50 mg/L

The adsorption percentage %R (Q) was calculated using equation 3 and the adsorption capacity (q) was calculated using equation 4. The distribution coefficient (K_d) was calculated using equation 5.

$$Q = \frac{C_o - C_e}{C_o} \times 100 \quad (3)$$

$$q_e = \frac{C_o - C_e}{m(g)} \times V(L) \quad (4)$$

$$K_d = \frac{C_o - C_e}{C_e} \times \frac{V(mL)}{m(g)} \quad (5)$$

where, C_o and C_e represent the initial and equilibrium concentrations respectively, V is the volume of the batch solution in liters or millilitres and m is the adsorbent weight in grams.

3.3 Effect of contact time

To each of the eleven sample tubes (50 mL volume with a screw led), 4.0 mL of the stock uranyl solution was transferred. The procedure was carried out as mentioned above for a contact time between 30 and 4320 minutes, after which the absorbance was measured. Initially the adsorption coefficient (K_d) increased rapidly. Between 300 and > 4000 minutes the system reached equilibrium. Therefore, the rest of the experiments were carried out for 5 hours. A graph was plotted for contact time (minutes) vs log K_d values as shown in Figure 5. A similar behaviour was reported by El-Sheikh *et al* [17].

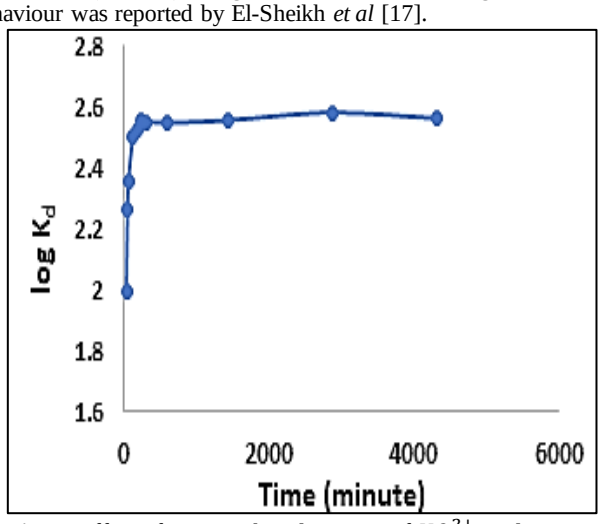

Fig. 5: Effect of time on the adsorption of UO_2^{2+} on diatomite.

3.4 Effect of pH:

As shown in Figure 6, the K_d value was almost stable at pH values between 2 and 4. Between 4 and 6 the curve shows a dramatic increase in K_d. At pH values between 6 and 7, K_d increased very slowly and a prompt increase was observed at pH 8. Above pH 8, the K_d decreased dramatically. This inconsistency can be attributed to the difference in uranyl ion species dominating the solution at different pH values. In the presence of carbon dioxide during batch experiments in addition to UO_2^{2+}, many other forms of uranyl hydroxides and carbonates such as: UO_2OH^+, UO_2CO_3, $UO_2(CO_3)_2^{2-}$ and $UO_2(CO_3)_2^{2-}$ can dominate at a different pH values above 5 [18, 19]. Therefore, the rest of the experiments were studied at pH 4.5.

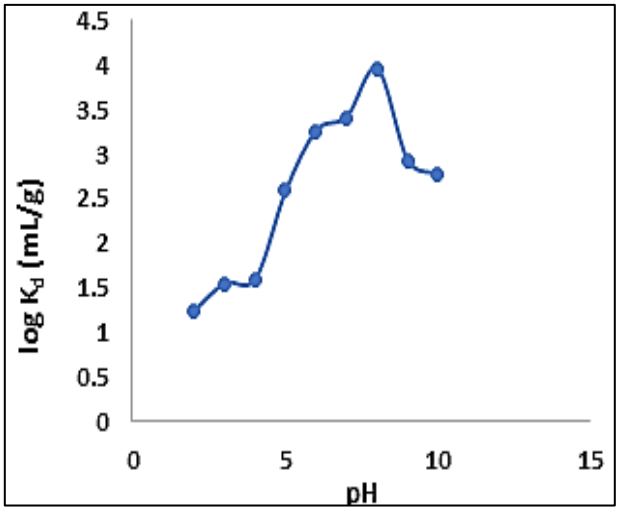

Fig. 6: Effect of pH change on the adsorption of uranyl ions on diatomite

3.5 Effect of initial ion concentration

The effect of the initial ion concentration was studied at 50-200 ppm, pH 4.5 and 2 g/L adsorbent. As shown in Figure 7, K_d decreases with increasing uranyl ion concentration. This is attributed to the fact that as the metal ion concentration increases, the number of negative sites on the adsorbent surface decreases. Therefore, the metal ion can not find enough active sites and the system will be saturated at a designated point. The distribution coefficient decreases from 3.3 at 50 ppm to 2.0 at 200 ppm of uranyl ions.

This means that the K_d value has negatively changed by approximately 33%. This was in agreement with that reported for the adsorption of ^{152}Eu on some kinds of minerals including diatomite [14]. This result is also in agreement with the adsorption of uranyl ions on kaolinite [10]. A similar behaviour was found for uranyl adsorption on fibrous cerium phosphate [9].

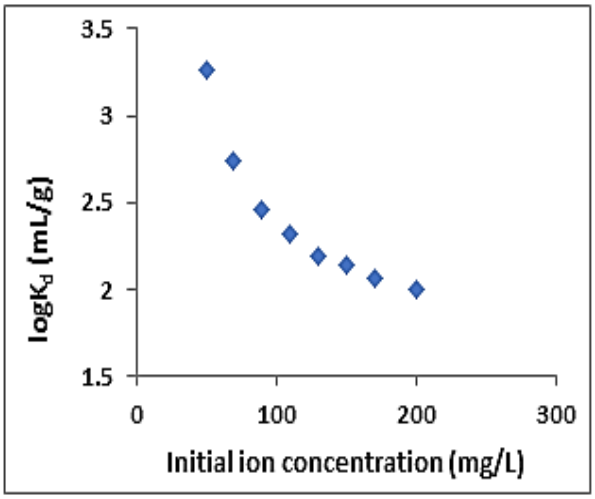

Fig. 7: Effect of uranyl ion concentration on the adsorption process on diatomite

3.6 Effect of adsorbent amount

To a series of uranyl ion solutions of 100 ppm at pH 4.5, was added a known amount of diatomite at a solid/liquid ratio of 0.5-5.0 g/L. Figure 8 shows that the adsorption percentage increased with increasing adsorbent amount. This is due to the increase in negative sites on the surface of the diatomite as the OH^- group increases. It is clear that the adsorption percentage (%R) increased from 27% at 0.5 g/L adsorbent amount to 54% when the adsorbent amount reached 5g/L. Figure 9 also shows that, from 0.5 g/L to 3 g/L, %R changes by 20%, while from 3 g/L to 5 g/L it changes only by 7%. This means that, the metal ions can occupy more sites on the surface of the adsorbent at lower solid/liquid ratios. This behaviour is expected, and has been observed for the adsorption of uranyl ions on kaolinite [10]; uranyl ions on fibrous cerium phosphate [9] and uranyl ions on Mesoporous Carbon Impregnated with Tri octylamine [20]. The adsorption capacity (q) decreases from 54 to mg/g with increasing adsorbent amount as shown in Figure 9.

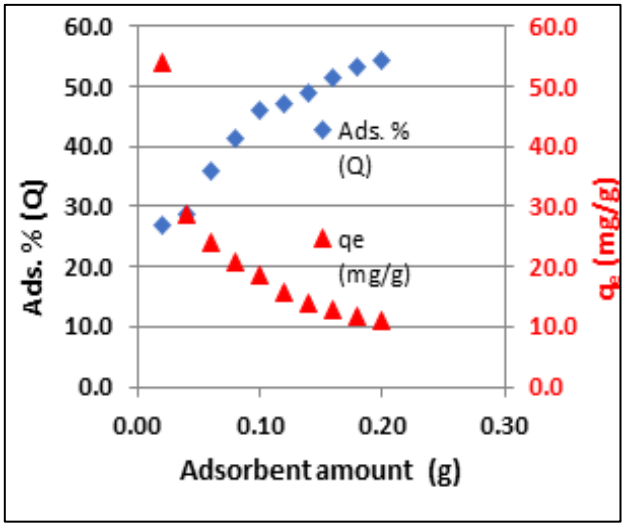

Fig. 8: Effect of diatomite dose on the adsorption of uranyl ions on diatomite

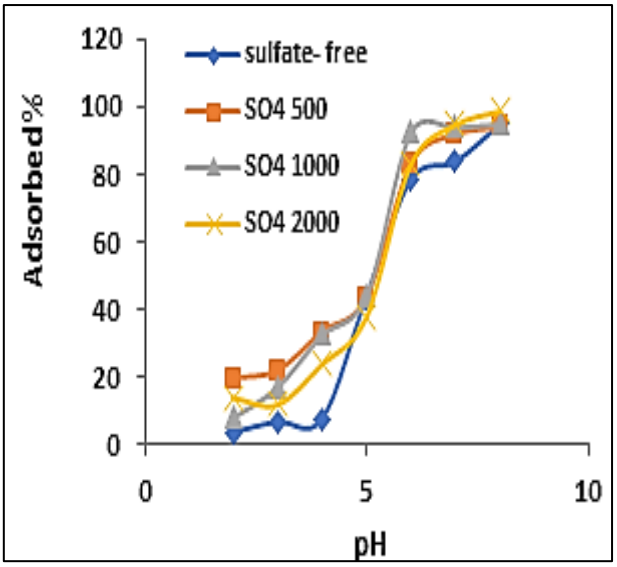

Fig. 9: Effect of sulfate ions on the adsorption of uranyl ions.

3.7 Effect of Sulfate ions

Adsorption of uranyl ions on diatomite minerals in the pH range from 2 to 8 was studied in the presence of sulfate ions (0, 500, 1000 and 2000 ppm) as shown in Figure 9. At pH<4, sulfate ions slightly enhance the adsorption of uranyl ions, regardless the order of sulfate ion concentration. In the presence of 500 ppm sulfate ions the adsorbed percentage increased from 3.4% to 19% at pH 2, but it increased from 7.3% to 32.5% at pH 4. At pH 3-4, the effect of sulfate ion concentration was in the order of 500 ppm≥1000 ppm>2000 ppm>sulfate free.

At higher basic media (i.e pH>7) the effect of sulfate ion concentration was insignificant according to Bachmaf et al. [21]. They found that sulfate of approximately 500ppm can reduce the sorption of uranyl (12 ppm) onto bentonite, and they assumed that this effect was due to the formation of a uranyl-sulfate complex or because of a competition between uranyl ion and sulfate in acidic media. However, they studied the behaviour in the presence of a NaCl solution, while our work was performed without any electrolyte solution. In another study on the sorption of uranyl (IV) above 2000ppm on hydrous oxides (e.g TiO_2, ThO_2 and CeO_2), the authors concluded that anions lsuch as nitrate, chloride and carbonate, reduced the sorption of uranyl ions, while sulfate ions in some cases increased the adsorption of uranyl ions which proposed to be due to uranyl-sulfate complex formation [22].

4. Adsorption modelling

An adsorption isotherm, which is a useful curve, often describes the mechanisms governing the retention (or release) or mobility of a chemical from aqueous porous media or aquatic habitats to a solid phase at a constant temperature and pH value [10]. The executed batch experiments yielded equilibrium isotherms for UO_2^{2+} ions. Following the optimization of the pH in 40 mL aliquots of 100 ppm uranyl ion,

various concentrations of diatomite (0.5 to 5.0 g/L) were applied. Equation 2 was used to determine the adsorption capacity or quantity of adsorbed UO_2^{2+} in mg per unit mass of adsorbent (g) in accordance with the Langmuir isotherm.

The Freundlich isotherm is based on the idea that the adsorbate adheres to the heterogeneous surface of an adsorbent and is relevant to both monolayer (chemisorption) and multilayer adsorption (physisorption). This model effectively depicts the adsorption data at low and intermediate concentrations on heterogeneous surfaces and allows for a wide variety of adsorption sites on the solid surface [23]. Equation 1 is the linear Freundlich equation.

$$log\, q_{max} = log K_F + \frac{1}{n} log C_o \qquad (1)$$

By plotting log $\mathbf{q_e}$ vs. log C_e, the value of the Freundlich constant ($\mathbf{K_F}$) was determined and found to be 2.0 $mg^{1-(1/n)}L^{1/n}g^{-1}$, and n, an empirical parameter reflecting the adsorption favourability (L/g) was found to be 1.00. C_o is the initial concentration (mg/L), and K_F and n are related to the adsorption capacity (q_{max}) and adsorption intensity, respectively.

The Temkin isotherm is frequently used for environmental research, and can be expressed by equation 2. where, q = solid-phase concentration, c = equilibrium liquid-phase concentration, R = gas constant, K_T = temperature, and b_T = adjustable parameters [14].

$$q = \frac{RT}{b_T} ln(K_T c) \qquad (2)$$

4.1 Langmuir isotherm

Equation 6 was used to apply the Langmuir model to describe the isotherm, where q_{max} (mg/g) represents the maximum adsorption capacity of the uranyl ion on diatomite, and K_L (L/mg) represents a constant that is indirectly related to the adsorption energy and describes the attraction between the adsorbate (metal ion) and the adsorbent (mineral). Equation 6 represents the Langmuir model in a linear version [24, 25]. This model is based on the premise that sorption occurs at specified homogenous locations within the sorbent material, which is supported by Langmuir's theory.

$$\frac{C_e}{q_e} = \frac{C_e}{q_{max}} + \frac{1}{q_{max} \times K_L} \qquad (6)$$

The slope and intercept of the linear equation (eq. 7) were used to obtain the Langmuir constant (K_L) to match the plot of Ce/qe vs Ce; see equations 8 and 9.

$$y = mx + c \qquad (7)$$

$$q_{max} = \frac{1}{slope} \qquad (8)$$

$$K_L = \frac{1}{q_{max} \times intercept} \qquad (9)$$

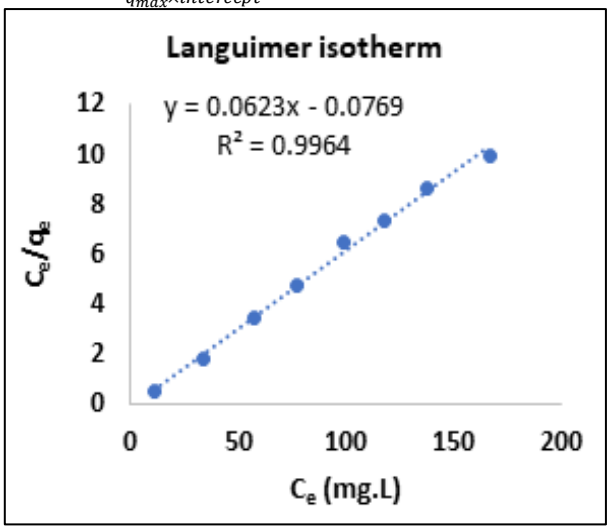

Fig. 10: Langmuir isotherm model for UO_2^{2+} ion on kaolinite

According to Suleyman [24], the correlation constant R^2 for diatomite is 0.9964, which indicates that the Langmuir model adequately describes the adsorption data and yields a maximum adsorption capacity of 16 mg/g. This claim describes the monolayer adsorption behaviour UO_2^{2+} on diatomite (Figure 10). The maximum adsorption capacity of uranyl on diatomite was greater than that for uranyl ions adsorbed on kaolinite as reported earlier [10].

The maximum distribution coefficient of UO_2^{2+} ions on diatomite was 3.3 at initial uranyl ion concentration of 50 mg/L (Figure 8). According to the Langmuir model, the equilibrium adsorption constant (K_L), which is related to binding affinity, is equal to 0.813 L/mg. The maximum uranium content per unit mass of diatomite for complete mono-layer coverage (q_{max}) is 16 mg/g. The separation factor (R_L) was found to be 0.0122 which means that the adsorption was favourable where RL is calculated according to equation 10.

$$R_L = \frac{1}{(1+C_o \times K_L)} \qquad (10)$$

4.2 Freundlich isotherm

The Freundlich isotherm behaviour of the uranyl ion on diatomite is depicted in Figure 11. The Freundlich model appears to adequately reflect the adsorption data because the correlation constant (R^2) for diatomite is 1.00, the adsorption capacity (K_F) is equal to 2.00, and the adsorption intensity (1/n) is equal to 1.00 [26]. This claim describes the behaviour of the UO_2^{2+} ion during monolayer and multilayer adsorption on diatomite. According to equation 4, the adsorption capacity was found to be 200 mg/g.

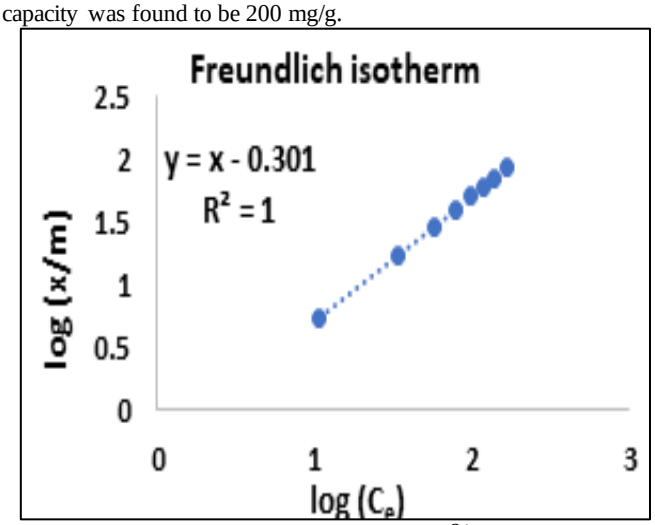

Fig. 11: Freundlich isotherm model for UO_2^{2+} ions on diatomite

4.3 **Temkin isotherm**

As shown in equation 5, for the Temkin model isotherm, $\mathbf{K_T}$ is the Temkin isotherm equilibrium binding constant (L/g); $\mathbf{b_T}$ is the Temkin isotherm constant and **R** is the universal gas constant (8.314 J/mol.K); **T** is the absolute temperature (298K). From the Temkin plot given in Figure 12, the following values were estimated: R^2=0.789, K_T= 0.9405 L/g and b_T= 24.724 J/mol, where b_T equals the slope and K_T =exp(intercept/b_T). Temkin has an endothermic adsorption isotherm which is less than Langmuir and Freundlich isotherms.

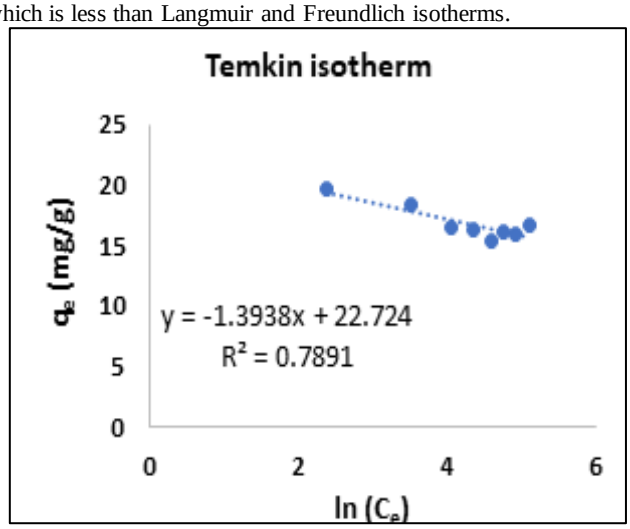

Fig. 12: Temkin isotherm for the adsorption of uranyl ions on diatomite.

5. Conclusion

In this work, adsorption behaviour of uranyl ions on natural diatomite was studied at different pH values, contact times, adsorbent masses, initial concentrations and ionic strengths. The suitable equilibrium time was 5 hours. The suitable pH for the maximum removal of uranyl ions on diatomite was 4.5, the contact time 5 hrs and the adsorbent dosage was 2 g/L. The Langmuir and Freundlich isotherms exhibited a very good fit and exothermic adsorption, while the Temkin isotherm

exhibited endothermic adsorption behavior and fit less well than did the other two isotherms.

6. Acknowledgement

Authors would kindly appreciate the Libyan Advanced Centre for Chemical Analysis for providing the laboratory facilities to do the research.

7. Reference

[1]- Zhang B. Zhu, Song Z., F., Guo Z., and Liu B. Efficient Removal of U(VI) Ions from Aqueous Solutions by Tannic Acid/Graphene Oxide Composites, *Appl. Sci. 2020, 10, 8870, pp 1-12; doi:10.3390/app10248870, http://www .mdpi.com/journal/applsci.*

[2]- Ikeda-Ohno A., Harrison, J.J.; Thiruvoth, S.; Wilsher, K.; Wong, H.K.Y.; Johansen, M.P.; Waite, T.D.; and Payne, T. Solution Speciation of Plutonium and Americium at an Australian Legacy, *Radioactive Waste Disposal Site. Environ. Sci. Technol. 2014, 48, 10045–10053*

[3]- C. Ding, C., Cheng, W., Sun Y., Wang X., Novel fungus-Fe_3O_4 bio-nanocomposites as high-performance adsorbents for the removal of radionuclides. *J. Hazard. Mater. 2015, 295, 127–137.*

[4]- Zhu K., Lu S., Gao, Y., Zhang R., Tan X., and Chen C., Fabrication of hierarchical core-shell polydopamine@ MgAl-LDHs composites for the efficient enrichment of radionuclides. *Appl. Surf. Sci., 2017, 396, 1726–1735.*

[5]- Mahmoud M. R., Soliman M. A., and Rashad G. M., Performance appraisal of foam separation technology for removal of Co(II)-EDTA complexes intercalated into in-situ formed Mg-Al layered double hydroxide from radioactive liquid waste. *Chem. Eng. J. 2017, 326, 781–793.*

[6]- Tokar E., Tutov M., Bratskaya S., Egorin A., Removal of Cs-137 Radionuclide by Resorcinol–Formaldehyde Ion-Exchange Resins from Solutions Simulating Real Liquid Radioactive Waste. Molecules *2022, 27, 8937, pp 1-17; https://doi.org/10.3390/molecules27248937.*

[7]- Chen B., Yu S., & Zhao X., The Separation of Radionuclides and Silicon from Boron-containing Radioactive Wastewater with Modified Reverse Osmosis Membranes. Process Safety and Environmental Protection. Volume 146, February 2021, Pages 639-646 *doi:10.1016/j.psep.2020.11.023.*

[8]- Sofronov D., Krasnopyorova A., Efimova N., Oreshina A., Bryleva E., Yuhno G., Lavrynenko S., and Rucki M., Extraction of radionuclides of cerium, europium, cobalt and strontium with Mn3O4, MnO_2, and MNOOH sorbents Process. *Saf. Environ. Prot. 2019, 125, 157–163.*

[9]- AlHanash H. B., Issa R. A. M., AlJabo H. A., (2022) Adsorption of UO_2^{2+} on Fibrous Cerium Phosphate and its Alanine and Arginine Intercalated Materials, *Academic Journal of Chemistry, (2022) Vol. 7, Issue, 4. pp: 47-54.*

[10]- Issa R. A. M., El Amari A. O., AlHanash H. B., Etmimi H. M., Removal of uranium (VI) ion from aqueous solution using kaolinite, *Kuwait Journal of Science, (2023) https://doi.org/10.1016/j.kjs.2023.03.010*

[11]- Kazan I., Silicaceous Rock of the USSR (Diatomites, Opokas, Tripolis, Spongiolites, Radiolarites) [in Russian], *Tatarskoe Knizhn, (1976).*

[12]- Ivanov S. E., and Belyacov A. V., Diatomite and its applications, *Glass and Ceramics, (2008) vol. 65, pp. 49-51.*

[13]- Sheng G. D., Shao D. D., Fan Q. H., Xu D., Chen Y. X., and Wang X. K., Effect of pH and ionic strength on sorption of Eu(III) to MX-80 *bentonite*: batch and XAFS study, *Radiochim. Acta (2009) 97, 621–630.*

[14]- Chu K. H., Revisiting the Temkin Isotherm: Dimensional Inconsistency and Approximate Forms. *Industrial & Engineering Chemistry Research, (2021) 60(35), 13140–13147. doi:10.1021/acs.iecr.1c01788*

[15]- Issa R. A. M., Ph. D. theses, University of Manchester, UK, (2013).

[16]- Al-Degs Y., Khraisheh M. A. M., Tutunji M. F., Sorption of lead ions on diatomite and manganese oxides modified diatomite, *Water Res., (2001) 35: 3724-3728.*

[17]- El-Sheikh A. S., Haggag E. A., and Abd El-Rahman N. R., Adsorption of Uranium from Sulfate Medium Using a Synthetic Polymer; Kinetic Characteristics, ISSN 1066-3622, Radiochemistry, 2020, Vol. 62, No. 4, pp. 499–510. Pleiades Publishing, Inc.

[18]- Markich S. J., Uranium Speciation and Bioavailability in Aquatic Systems: An Overview, *The Scientific World JOURNAL (2002) 2, 707-729 ISSN 1537-744 X; DOI 10.1100/tsw.2002.130.*

[19]- Mühr-Ebert E. L., Wagner F., Walthe C., Speciation of uranium: Compilation of a thermodynamic database and its experimental evaluation using different analytical techniques, Applied Geochemistry (2019) 100, 213-222.

[20]- Morsy A. M. A., and Ali A. H., Sorption of Uranium from Waste Effluent Solutions by Mesoporous Carbon Impregnated with Tri octylamine, *RADIOCHEMISTRY Vol. (2017) 59 No. 2 pp 135-141*

[21]- Bachmaf S., Planer-Friedrich B., and Merkel B. J., Effect of sulfate, carbonate, and phosphate on the uranium (VI) sorption behavior onto bentonite. *Radiochimica Acta, (2008) 96(6). doi:10.1524/ract.2008.1496*

[22]- Mahal H. S., Venkatarmani B., and Venkateswarlu K. S., Sorption properties of oxides IX: effect of anions one the sorption of uranium (VI) hydrous oxides, *Proc. India Acad. (Chem. Sci.), Vol. 91, No. 4, August 1982, pp 321-327.*

[23]- Boparai H. K., Joseph M., and O'Carroll D. M., Kinetics and thermodynamics of cadmium ion removal by adsorption onto nano zerovalent iron particles, Journal of Hazardous Materials (2011) 186 (2011) 458–465

[24]- Langmuir I., The adsorption of gases on plane surfaces of glass, mica and platinum. *Journal of the American Chemical Society 1918; 40: 1361-1403.*

[25]- Suleyman I., Sorption of europium on cerium phosphate using Box-Behnken design, *Turk J Chem., 2020; 44: 971-986.*

[26]- Akl Z. F., Theoretical and experimental studies on uranium(vi) adsorption using phosphine oxide-coated magnetic nanoadsorbent, RSC Adv., 2021,11, 39233-39244